Original Article

http://www.jcpjournal.org
pISSN 2288-3649 · eISSN 2288-3657
https://doi.org/10.15430/JCP.2020.25.2.100

JCP

15-Deoxy-$\Delta^{12,14}$-prostaglandin J_2 Induces Apoptosis in Ha-*ras*-transformed Human Breast Epithelial Cells by Targeting IκB kinase–NF-κB Signaling

Hye-Kyung Na[1,2], Hongkyung Yang[2], Young-Joon Surh[3]

[1]Department of Food Science and Biotechnology, College of Knowledge-Based Services Engineering, Sungshin Women's University, [2]Department of Future Applied Sciences, College of Natural Sciences, Sungshin Women's University, [3]Tumor Microenvironment Global Core Research Center, College of Pharmacy, Seoul National University, Seoul, Korea

15-Deoxy-$\Delta^{12,14}$-prostaglandin J_2 (15d-PGJ_2), an endogenous ligand for PPARγ, has differential effects on cancer cell proliferation and survival depending on the dose and the type of cells. In the present study, we have investigated the effects of 15d-PGJ_2 on apoptosis of the Ha-*ras* transformed human breast epithelial (MCF10A-*ras*) cells. When MCF10A-*ras* cells were treated with 15d-PGJ_2 (10 μM) for 24 hours, they underwent apoptosis as evidenced by characteristic morphological features, an increased proportion of sub-G_0/G_1 cell population, a typical pattern of annexin V/propidium iodide staining, perturbation of mitochondrial transmembrane potential ($\Delta\psi_m$), and cleavage of caspase-3 and its substrate PARP. A pan-caspase inhibitor, Z-Val-Ala-Asp (OCH_3)-fluoromethyl ketone attenuated cytotoxicity and proteolytic cleavage of caspase-3 induced by 15d-PGJ_2. The 15d-PGJ_2-induced apoptosis was accompanied by enhanced intracellular accumulation of reactive oxygen species (ROS), which was abolished by the antioxidant *N*-acetyl-L-cysteine (NAC). 15d-PGJ_2 inhibited the DNA binding activity of NF-κB which was associated with inhibition of expression and catalytic activity of IκB kinase β (IKKβ). 15d-PGJ_2-mediated inhibition of IKKβ and nuclear translocation of phospho-p65 was blocked by NAC treatment. 9,10-Dihydro-PGJ_2, a non-electrophilic analogue of 15d-PGJ_2, failed to produce ROS, to inhibit NF-κB DNA binding, and to induce apoptosis, suggesting that the electrophilic α,β-unsaturated carbonyl group of 15d-PGJ_2 is essential for its pro-apoptotic activity. 15d-PGJ_2-induced inactivation of IKKβ was also attributable to its covalent thiol modification at the cysteine 179 residue of IKKβ. Based on these findings, we propose that 15d-PGJ_2 inactivates IKKβ–NF-κB signaling through oxidative or covalent modification of IKKβ, thereby inducing apoptosis in Ha-*ras* transformed human breast epithelial cells.

Key Words 15-Deoxy-$\Delta^{12,14}$-prostaglandin J_2, Apoptosis, Reactive oxygen species, IKKβ–NF-κB, MCF10A-*ras* cells

INTRODUCTION

An endogenous ligand for PPARγ, 15-deoxy-$\Delta^{12,14}$-prostaglandin J_2 (15d-PGJ_2) is a cyclopentenone prostaglandin formed via two step dehydration of prostaglandin D_2. 15d-PGJ_2 has been known to exert diverse biological activities such as pro-inflammatory/anti-inflammatory, carcinogenic/anti-carcinogenic, and prooxidant/anti-oxidant effects, depending on the types of cells and the concentration used [1]. It has been shown that synthetic PPARγ ligands as well as 15d-PGJ_2 can induce growth inhibition, apoptosis, and terminal differentiation of several types of cancerous and transformed cells. 15d-PGJ_2 attenuated the capability of the MDA-MB-231 cells to induce xenograft tumors in nude mice [2]. In addition, 15d-PGJ_2 inhibits migration of breast cancer MDA-MD-231 cells and osteolytic breast cancer bone metastasis in nude mice [2]. 15d-PGJ_2 inhibits phorbol ester-induced expression of matrix metallopeptidase-9 and invasion of MCF-7 cells [3]. Moreover, 15d-PGJ_2 synergistically enhanced the anti-tumor activity of the chemotherapeutic agent doxorubicin in renal cell carcinoma [4], and markedly reduced growth of murine colorectal carcinoma and HL-60 leukemia xenograft tumors [5].

The anti-proliferative effects of 15d-PGJ_2 are associated with de novo synthesis of proteins involved in regulating the cell cycle and apoptosis. 15d-PGJ_2 inhibited c-myc, cyclin D2, and cyclin D1 expression with concomitant induction of $p21^{waf1}$ and $p27^{kip1}$ in various type of cancer cells [6,7]. In

Received June 22, 2020, Revised June 24, 2020, Accepted June 24, 2020
Correspondence to Hye-Kyung Na, E-mail: nhk1228@sungshin.ac.kr, https://orcid.org/0000-0003-0460-2810

addition, 15d-PGJ_2 has been reported to induce apoptosis in diverse types of cancer cells, including gastric, colorectal, osteosarcoma, pancreatic, breast cancer [5,8-11]. 15d-PGJ_2-induced apoptosis was associated with production of reactive oxygen species (ROS) [9] and mediated by regulating expression levels of the Bcl-2 family member proteins, such as Bax and Bcl-2 [8,12] and by downregulation of SIRT1 [13].

Although 15d-PGJ_2 was first identified as an endogenous PPARγ ligand, its biological effects are mainly achieved by PPARγ-independent mechanisms through direct interaction with diverse signaling molecules and their regulators. 15d-PGJ_2 has a reactive α,β-unsaturated carbonyl group in the cyclopentane ring which reacts with nucleophilic cellular moiety such as cysteine and hence covalently modifies and regulates the activation of the redox proteins [14]. For instance, 15d-PGJ_2 directly binds to c-Jun at a specific cysteine residue located in the DNA binding domain of AP-1, thereby inactivating this transcription factor [15]. Furthermore, it has been known that 15d-PGJ_2 induces expression of phase II detoxification or antioxidant enzymes through Nrf2 activation, which may confer cellular defense against or adaptation to carcinogenic insult or oxidative stress [16]. Also, 15d-PGJ_2 directly inhibits NF-κB-dependent gene expression through covalent modifications of critical cysteine residues in IκB kinase (IKK) [17,18] and the DNA-binding domains of NF-κB subunits [18,19]. The inhibitory effect of 15d-PGJ_2 on NF-κB signaling through thiol modification of NF-κB may contribute to anti-inflammatory and anti-proliferative effects through inhibition of target gene expression such as Bcl-2. In this study, we investigated pro-apoptotic activity of 15d-PGJ_2 in Ha-*ras* transformed human breast epithelial cells with focus on IKKβ–NF-κB axis as a potential target.

MATERIALS AND METHODS

Materials

15d-PGJ_2 and 9,10-dihydro15d-PGJ_2 (H2-15d-PGJ_2) were purchased from Cayman Chemical Co. (Ann Arbor, MI, USA). Dulbecco's modified Eagle's medium (DMEM)/F-12, heat-inactivated horse serum, L-glutamine, penicillin/streptomycin/fungizone mixture were products of Gico BRL (Grand Island, NY, USA). MTT, insulin, cholera toxin, hydrocortisone, recombinant epidermal growth factor, *N*-Acetyl-L-cysteine (NAC), dithiothreitol (DTT), propidium iodide (PI), N-benzyloxycarbonyl-Val-Ala-Asp-fluoromethylketone (zVAD-FMK), and anti-actin antibody were purchased from the Sigma-Aldrich Co. (St Louis, MO, USA). 2',7'-Dichlorodihydrofluorescein diacetate (DCF-DA) was purchased from Calbiochem (San Diego, CA, USA). Annexin V-FITC staining agent was supplied by Biosciences Pharmingen (Franklin Lakes, NJ, USA). Tetramethylrhodamine ethyl ester (TMRE) was obtained from Molecular Probes, Inc. (Eugene, OR, USA). [γ-^{32}P]ATP was the product of NEN Life Science (Boston, MA, USA). Antibodies against cleaved PARP and cleaved-caspase 3 were purchased from Cell Signaling Technology (Beverly, MA, USA). IKKβ and pp65 antibodies were from Santa Cruz Biotechnology (Santa Cruz, CA, USA). Secondary antibodies and FITC-conjugated goat anti-rabbit immunoglobulin G (IgG) were obtained from Zymed Laboratories Inc. (San Francisco, CA, USA). The protein G agarose bead was purchased from Invitrogen (Carlsbad, CA, USA). The enhanced chemiluminescence detection reagent was purchased from Amersham Co. (Arlington Heights, IL, USA). IKKβ (wild type) and its mutant construct IKKb (C179A) were kindly provided by professor Dae Myung Jue from The Catholic University of Korea. 15d-PGJ_2 was dissolved in dimethyl sulfoxide (DMSO) and diluted further in culture medium.

Cells culture

The MCF10A-*ras* cell line was kindly provided by Prof. Aree Moon of Duksung Women's University, Seoul, South Korea. The cells were cultured in DMEM: Nutrient Mixture-F-12 (DMEM/F-12) supplemented with 5% heat-inactivated horse serum, 10 μg/mL insulin, 100 ng/mL Cholera toxin, 0.5 μg/mL hydrocortisone, 20 ng/mL recombinant epidermal growth factor, 2 mM L-glutamine, 100 μg/mL penicillin/streptomycin/fungi zone mixture at 37°C in a 5% CO_2 atmosphere.

Cell growth assay

MCF10A-*ras* cells were plated at a density of 4×10^4 cells in 48-well plates, and the cells were treated with different concentrations of 15d-PGJ_2 for 24 hours. The cell viability was determined by the conventional MTT reduction assay. After treatment with 15d-PGJ_2, the cells were treated with the MTT solution (final concentration, 0.25 mg/mL) for 2 hours at 37°C in a 5% CO_2 atmosphere. The dark blue formazan crystals formed in intact cells were dissolved with DMSO and the absorbance was measured at 570 nm using a microplate reader. Results were expressed as the percentage of MTT reduction obtained in the treated cells, assuming that the absorbance of control cells was 100%. All samples were prepared in triplicates.

Annexin V-FITC staining

To quantify the percentage of cell population that are actively undergoing apoptosis, Annexin V-FITC was used according to manufacturer's protocol. Briefly, MCF10A-*ras* cells plated at a density of 2×10^5 cells in 6-well plates were treated with 15d-PGJ_2 in the presence or absence of NAC for 12 hours. Phosphatidylserine externalization was detected with FACScalibur instrument after staining with an impermeable dye Annexin V-FITC according to the instructions provided from the supplier.

Measurement of sub-diploid DNA and DNA distribution

MCF10A-*ras* cells were plated at a density of 2 × 10^5 cells in 6-well plates, and the cells were treated with 15d-PGJ_2 in the presence or absence of NAC for 12 hours. Adherent and detached cells were washed, trypsinized, collected by centrifuged at 1,300 rpm for 5 minutes, and fixed with 1 mL of 70% cold ethanol. Fixed cells were stored at –20°C until use it. After centrifuge at 2,100 rpm for 10 minutes, the fixed cells were stained with PBS containing 0.1% Triton X-100, 0.1 mM EDTA (pH 7.4), 10 μg/mL RNase A, 50 μg/mL PI and 10,000 cells per sample were analyzed by a FACScalibur instrument (BD Biosciences, San Jose, CA, USA) as described previously [20]. The DNA histograms were further analyzed by Cell Quest Pro Software to calculate the proportion of sub-diploid cell population.

Measurement of mitochondrial transmembrane potential

To measure the mitochondrial transmembrane potential ($\Delta\psi_m$), the lipophilic cationic probe TMRE was used. MCF10A-*ras* cells were cultured in 4 chamber slide glasses. After treatment, the cells were rinsed with PBS and incubated with TMRE (150 nM) in the fresh media for 30 minutes at 37°C. The cells were examined under a confocal microscope (Leica Microsystems Heidelberg GmbH, Heidelberg, Germany) with the fluorescence excitation at 488 nm and emission at 590 nm.

Measurement of intracellular ROS accumulation

To monitor net intracellular accumulation of ROS, the fluorescence generating probe DCF-DA was used. MCF10A-*ras* cells were cultured in 4 chamber slide glasses. After treatment with 15d-PGJ_2 (10 μM) or vehicle at 37°C for 12 hours, the cells were washed with PBS and incubated with DCF-DA (10 μM) in a fresh medium for additional 15 minutes in the dark. The cells were examined under a confocal microscope (Leica Microsystems Heidelberg GmbH) with the fluorescence excitation at 488 nm and emission at 530 nm. The integrated density of 3 captured scenes of each treatment was measured using the Adobe Photoshop CS5 program (Adobe Inc., San Jose, CA, USA).

Transient transfection

MCF10A-*ras* cells seeded at a density of 2 × 10^5/well in a 6-well dish were grown to 60%-70% confluence in complete growth media. The cells were transfected with 2 μg of pFlag-CMV2-IKKβ (wild type) or its mutant construct IKKβ (C179A) using DOTAP liposomal transfection reagent (Roche Applied Science, Mannheim, Germany) according to the manufacturer's instructions. After 12-hour transfection, the cells were treated with 15d-PGJ_2 or DMSO in the presence or absence of DTT for additional 12 hours and then washed with PBS and digested with lysis buffer (Promega, Madison, WI, USA) for Western blot analysis and the kinase assay.

IKK kinase assay

MCF10A-*ras* cells were cultured in 100-mm dishes in the absence or presence of 15d-PGJ_2. When necessary, DTT (500 μM) was added. The protein was isolated as described above for the Western blot analysis. The lysed cell extract (200 μg) was precleared using normal mouse immunoglobulin G and protein G agarose beads and subjected to immunoprecipitation by using anti-IKKβ antibody. The resulting immunocomplex was pulled down by mixing with protein G agarose beads. The immunoprecipitates were suspended in 50 μL of a reaction mixture containing 1X kinase buffer (Cell Signaling Technology, Beverly, MA, USA), 1 μg glutathione *S*-transferase-IκBα as a substrate and 10 μCi of [γ-^{32}P]ATP and incubated at 30°C for 45 minutes. The kinase reaction was terminated by adding SDS loading dye, boiled for 5 minutes at 99°C, vortexed and centrifuged at 5,000 rpm for 2

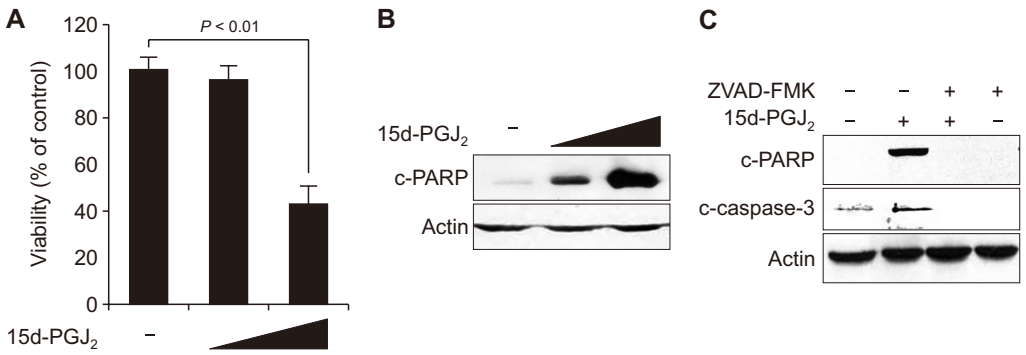

Figure 1. 15-Deoxy-Δ^{12,14}-prostaglandin J_2 (15d-PGJ_2) induced apoptosis in MCF10A-*ras* cells. (A, B) MCF10A-*ras* cells were treated with 15d-PGJ_2 (5 and 10 μM) for 24 hours. The cell viability was determined by the conventional MTT reduction assay. Bars represent mean ± SE of three experiments. A significant difference in the relative viability between treated cells and the solvent control is indicated with $P < 0.01$. (B) The proteolytic cleavage of PARP and actin were examined by Western blot analysis. (C) MCF10A-*ras* cells were treated with 15d-PGJ_2 (10 μM) for 24 hours in the presence or absence of an pan-caspase inhibitor N-benzyloxycarbonyl-Val-Ala-Asp-fluoromethylketone (ZVAD-FMK). Expression of cleaved PARP and caspase-3 was detected by Western blot analysis.

minutes. The supernatant was separated by 12% SDS-polyacrylamide gel. The gel was stained with Commassie Brilliant Blue G 250 and treated with destaining solution (glacial acetic acid:methanol:distilled water, 1 : 4 : 5, v/v). The destained gel was dried at 80°C for 1 hour and exposed to X-ray film to detect the phosphorylated glutathione *S*-transferase-$I\kappa B\alpha$ in the radiogram. Mouse immunoglobulin G heavy chain band that appeared on the destained gel was used as the loading control to ensure the equal lane loading.

Electrophoretic mobility shifty assay (EMSA)

MCF10A-*ras* cells were cultured in 100-mm dishes in the absence or presence of 15d-PGJ_2. Nuclear extracts from the cells were prepared as described previously [20]. The synthetic double strand oligonucleotide harboring the NF-κB binding domain was labeled with [γ-^{32}P]ATP using T4 polynucleotide kinase (Takara Korea Biomedical Inc., Daejeon, Korea) and purified by gel filtration using a nick spin column (Amersham Bioscience, Piscataway, NJ, USA). To ensure the specificity of the binding, a competition experiment was carried out by adding the excess unlabeled oligonucleotide to the reaction mixture prior to the labeled oligonucleotide. After determination of the protein concentration, DNA binding reaction for EMSA was processed according to the method previously reported [20].

Immunocytochemistry

MCF10A-*ras* cells were seeded at 3 × 10^4 cells per well in an 8 chamber slide. After fixation with 10% neutral-buffered formalin solution for 30 minutes at room temperature, MCF10A-*ras* cells were incubated with blocking agents (0.1% Tween-20 in PBS containing 5% bovine serum albumin [BSA]), washed with PBS and then incubated with a diluted (1 : 100) primary antibody for overnight at 4°C. After washing with PBS (twice for 5 minutes each), samples were incubated with a diluted (1 : 1,000) FITC-goat anti-rabbit IgG secondary

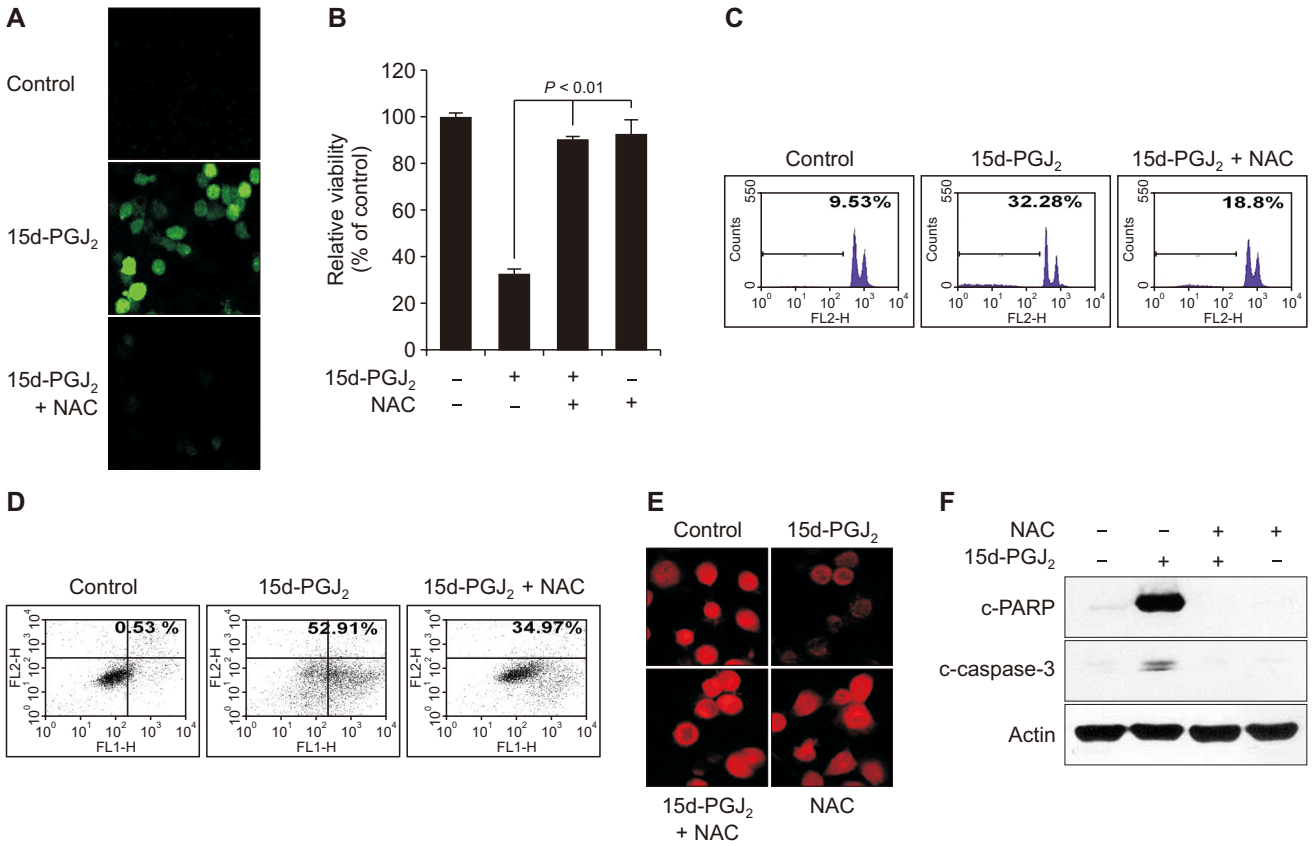

Figure 2. Reactive oxygen species (ROS) plays an important role in induction of apoptosis by 15-deoxy-$\Delta^{12,14}$-prostaglandin J_2 (15d-PGJ_2) in MCF10A-*ras* cells. MCF10A-*ras* cells were treated with 15d-PGJ_2 (10 μM) in the presence or absence of *N*-acetyl-L-cysteine (NAC) (5 mM) for 24 hours. (A) ROS production was determined by the 2',7'-Dichlorodihydrofluorescein diacetate staining. (B) Effects of NAC (5 mM) on 15d-PGJ_2-induced cytotoxicity was measured by the MTT assay. Bars represent mean ± SE of three independent assays. A significant difference in the relative viability between treated cells and the solvent control is indicated with $P < 0.01$. (C, D) The sub-G_0/G_1 population and the Annexin V-FITC/propidium iodide positive cell population were analyzed by flow cytometry. The values in each panel indicate the ratio of apoptotic cell population. (E) Mitochondrial membrane potential was determined by use of tetramethylrhodamine ethyl ester in the cells treated with 15d-PGJ_2 in the absence or presence of NAC (5 mM) for 24 hours. The cells were examined under a confocal microscope with the fluorescence excitation at 488 nm and emission at 590 nm. (F) Effect of NAC on 15d-PGJ_2-induced proteolytic cleavage of PARP and caspase-3.

antibody for 1 hour. This was followed by washing cells with PBS and incubation with PI. The signals were detected using a confocal microscope.

Western blot analysis

Treated MCF10A-*ras* cells were washed with cold PBS and digested with lysis buffer (150 mM NaCl, 0.5% Triton X-100, 50 mM Tris-HCl, pH 7.4, 25 mM NaF, 20 mM EGTA, 1 mM DTT, 1 mM Na_3VO_4, protease inhibitor cocktail tablet) for 15 minutes on ice followed by centrifugation at 12,000 ×*g* for 20 minutes. The protein concentration of the supernatant was measured by using the bicinchoninic acid reagents (Pierce, Rockfold, IL, USA). Protein (30 μg) was separated by running through 12% SDS-PAGE gel and transferred to the polyvinylidene fluoride membrane (Gelman Laboratory, Ann Arbor, MI, USA). The blots were blocked with 5% non-fat dry milk-PBS containing 0.1% Tween-20 (PBST) buffer for 1 hour at room temperature. Each membrane was incubated with corresponding primary antibodies in 3% non-fat dry milk-PBST or 3% BSA. Equal protein loading was assessed using actin. After three time rinse with PBST buffer, the blot was incubated with 1 : 5,000 dilution of the horseradish peroxidase conjugated-secondary antibody (Zymed Laboratories Inc.) for 1 hour. Immunoreactive protein complexes were detected by enhanced chemiluminescence detection reagent after washing the blot three times with PBST.

Statistical analysis

Values were expressed as the mean ± SE of at least three independent experiments. Statistical significance was determined by Student's *t*-test. The criterion for statistical significance was $P < 0.05$, $P < 0.01$, and $P < 0.001$.

RESULTS

15d-PGJ_2 induces apoptosis in MCF10A-*ras* cells

First, we determined the effect of 15d-PGJ_2 on viability of MCF10A-*ras* cells by the MTT assay. When MCF10A-*ras* cells were treated with 10 μM 15d-PGJ_2 for 24 hours, there was about 60% reduction in the cell viability (Fig. 1A). To determine whether the anti-proliferative effect of 15d-PGJ_2 was associated with apoptotic cell death, we measured cleavage-PARP, a hallmark of apoptosis. The proteolytic cleavage of PARP was evident in the MCF10A-*ras* cells treated with 15d-PGJ_2 (Fig. 1B). To determine whether 15d-PGJ_2-induced apoptosis was mediated by caspases, MCF10A-*ras* cells were co-treated with a pan-caspase inhibitor, zVAD-FMK. 15d-PGJ_2-induced proteolytic cleavage of caspase-3 and its substrate PARP was attenuated by zVAD-FMK treatment (Fig. 1C).

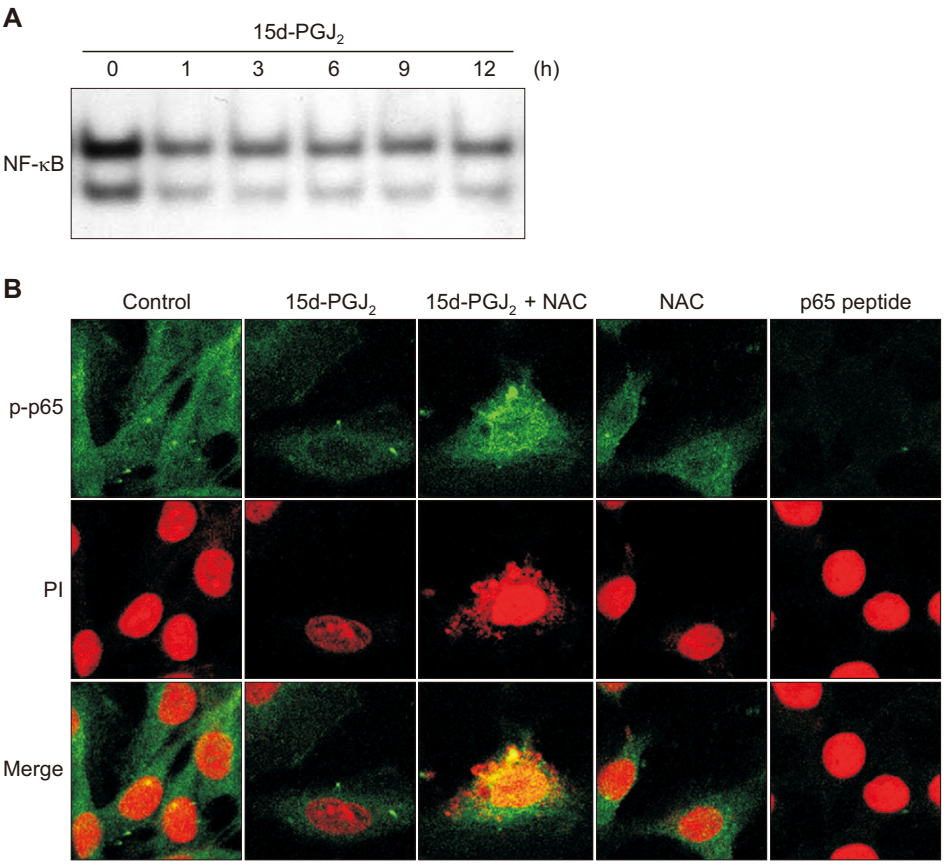

Figure 3. 15-Deoxy-$\Delta^{12,14}$-prostaglandin J_2 (15d-PGJ_2) suppresses the NF-κB DNA binding activity. (A) MCF10A-ras cells were treated with 15d-PGJ_2 (10 μM) for indicated time, and the nuclear protein was isolated. Nuclear extracts from MCF10A-*ras* cells were incubated with [γ-^{32}P]-labeled oligonucleotides harboring the NF-κB-consensus sequence. (B) MCF10A-*ras* cells were treated with 15d-PGJ_2 in the absence or presence of *N*-acetyl-L-cysteine (NAC) (5 mM) for 12 hours and immunocytochemical analysis was performed by using an antibody for phospho-p65. Propidium iodide (PI) was used to stain the nuclear of MCF10A-*ras* cells. The stained cells were analyzed under a confocal microscope.

15d-PGJ$_2$ induces intracellular ROS accumulation in MCF10A-*ras* cells

ROS is an universal entity mediating apoptosis in cancer cells [21]. To determine whether 15d-PGJ$_2$-induced apoptosis was attributable to generation of ROS, we utilized a fluorescent dye DCF-DA, capable of detecting peroxides including H_2O_2. 15d-PGJ$_2$ treatment led to an enhanced accumulation of ROS, which was attenuated by the general antioxidant NAC (Fig. 2A). NAC treatment attenuated 15d-PGJ$_2$-induced cytotoxicity (Fig. 2B), the proportion of sub-G_0/G_1 population (Fig. 2C) and apoptotic cells stained with Annexin-V/FITC (Fig. 2D). ROS generation is mediated by perturbation of mitochondrial membrane potential [22]. When MCF10A-*ras* cells were exposed to 15d-PGJ$_2$ (10 μM), the mitochondrial membrane became rapidly depolarized (Fig. 2E). Furthermore, proteolytic cleavage of caspase-3 and its substrate PARP induced by 15d-PGJ$_2$ was abrogated by NAC treatment in MCF10A-*ras* cells (Fig. 2F).

15d-PGJ$_2$-induced apoptosis is mediated through suppression of IKKβ

NF-κB has been known to be associated with resistance to apoptosis in various cancer cells [23]. 15d-PGJ$_2$ has been known to inhibit the NF-κB signaling [17]. The predominant form of NF-κB consists of p50 and p65 subunits that is sequestered in the cytoplasm by its inhibitory counterpart IκB-α. Signal dependent activation of IKK complex leads to the inducible phosphorylation of IκB proteins at two conserved serine residues located within their N-terminal region. Phospho-IκB proteins are ubiquitinated and subsequently degraded by the 26S proteasomes, leading to release of NF-κB from their inhibitory influence for translocation into the nucleus and transcriptional regulation of target genes, including Bcl-2.

IKK is a multi-subunit complex that contains two catalytic subunits, IKKα and IKKβ, and a regulatory subunit, IKKγ/NEMO (NF-κB essential modulator) [24]. Downregulation of IKKβ is associated with suppression of tumor development [25]. Therefore, targeting NF-κB and its activating kinase, IKK have become an appealing therapeutic strategy in the progression of many diseases including chronic inflammation and cancer [26].

To determine whether the 15d-PGJ$_2$-induced apoptosis was mediated by targeting the NF-κB pathway, we examined the effect of 15d-PGJ$_2$ on DNA binding activity of NF-κB. As shown in Figure 3A, 15d-PGJ$_2$ inhibited the NF-κB DNA binding activity. Phosphorylation of the p65 subunit has been considered to facilitate the translocation of NF-κB into nucleus. 15d-PGJ$_2$ treatment suppressed the localization of phospho-p65 into the nucleus which was blunted by co-treatment with NAC (Fig. 3B).

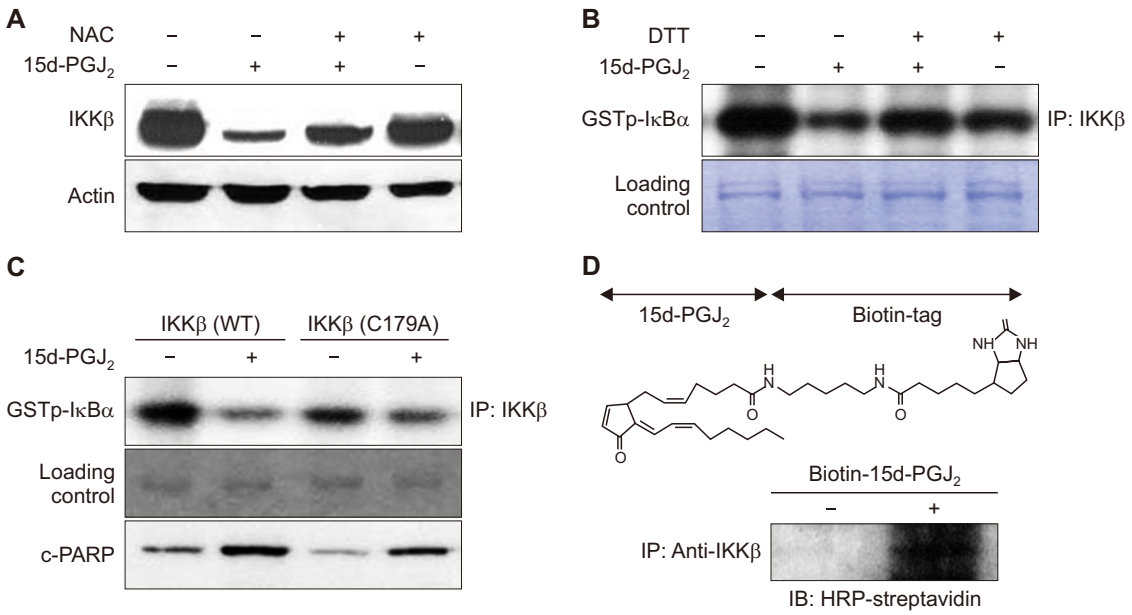

Figure 4. Downregulation of IKKβ is associated with induction of apoptosis in MCF10A-*ras* cells treated with 15-deoxy-Δ^{12,14}-prostaglandin J$_2$ (15d-PGJ$_2$). (A, B) MCF10A-*ras* cells were cotreated with *N*-acetyl-L-cysteine (NAC) (5 mM) or a thiol reducing agent, dithiothreitol (DTT) (500 μM), in the presence of 15d-PGJ$_2$ (10 μM) for 24 hours. The expression level of IKKβ was determined by Western blot analysis. The proteins were immunoprecipitated by anti-IKKβ and subsequently incubated with glutathione *S*-transferase-IκB-α and [γ-^{32}P]ATP for the kinase assay. Murine immunoglobulin G heavy chain band was used to ensure the equal lane loading. (C) MCF10A-*ras* cells were transfected with IKKβ and its mutant construct in which Cys179 is replaced by alanine. The catalytic activity of IKKβ and proteolytic cleavage of caspase-3 were determined by the kinase assay and Western blot analysis, respectively. (D) MCF10A-*ras* cells were treated with biotinylated 15d-PGJ$_2$ (10 μM) for 12 hours. The biotinylated 15d-PGJ$_2$-IKKβ complex was detected by the immunoprecipitation with IKKβ followed by Western blot analysis against horseradish peroxidase (HRP)-streptavidin as described in Materials and Methods.

In addition, 15d-PGJ_2 inhibited the expression and catalytic activity of IKKβ, which were attenuated by NAC and DTT, respectively (Fig. 4A and 4B). IKKβ has a cysteine residue at position 179 within its activation loop [17]. To determine whether this cysteine of IKKβ is critical for loss of its catalytic activity and subsequent induction of apoptosis by 15d-PGJ_2, we utilized a mutant IKKβ construct in which cysteine 179 is replaced by alanine. 15d-PGJ_2-induced suppression of IKKβ catalytic activity and proteolytic cleavage of PARP were less prominent in MCF10A-*ras* cells transfected with mutant IKKβ compared to those in cells harboring wild type IKKβ (Fig. 4C). These results suggest that 15d-PGJ_2-induced apoptosis is associated, in part, with inhibition of IKKβ through covalent modification at cysteine 179. To further verify that 15d-PGJ_2 could directly modify IKKβ, we utilized a biotinylated derivative of 15d-PGJ_2. In this experiment, MCF10A-*ras* cells were treated with biotinylated 15d-PGJ_2 and immunoprecipitated with anti-IKKβ, and the 15d-PGJ_2 bound to IKKβ was detected with horseradish peroxidase (HRP)-streptavidin. We have observed that biotinylated 15d-PGJ_2 directly bound to IKKβ, suggesting IKKβ as a critical potential target for 15d-PGJ_2-induced apoptosis (Fig. 4D).

In another experiment, a pharmacological inhibitor of IKKβ (Bay11-7082) increased the apoptotic cell population positive for Annexin V and proteolytic cleavage of caspase-3, which were suppressed by NAC treatment (Fig. 5A and 5B). Moreover, the pharmacologic inhibition of IKKβ suppressed the cell viability (Fig. 5C) as well as its catalytic activity (Fig. 5D), which were attenuated by NAC (Fig. 5C and 5D).

The α,β-unsaturated carbonyl moiety of 15d-PGJ_2 is essential for its induction of apoptosis in MCF10A-*ras* cells

The α,β-unsaturated carbonyl group in the cyclopentane ring of 15d-PGJ_2 renders it reactive towards cellular nucleophilics to form covalently bound Michael adducts. To determine whether the α,β-unsaturated carbonyl moiety of 15d-PGJ_2 plays an important role in induction of apoptosis in MCF10A-*ras* cells, we compared its effects with those of the non-electrophilic analogue, 9,10-dihydro-15d-PGJ_2 (Fig. 6A). We observed that 9,10-dihydro-15d-PGJ_2, lacking the α,β-unsaturated carbonyl moiety, failed to generate ROS (Fig. 6B) and to inhibit NF-κB DNA binding activity (Fig. 6C). In addition, 9,10-dihydro-15d-PGJ_2 did not enhance the proportions of sub-G_0/G_1 population and Annexin V positive cells as well as cytotoxicity in MCF10A-*ras* cells (Fig. 6D and 6E). More-

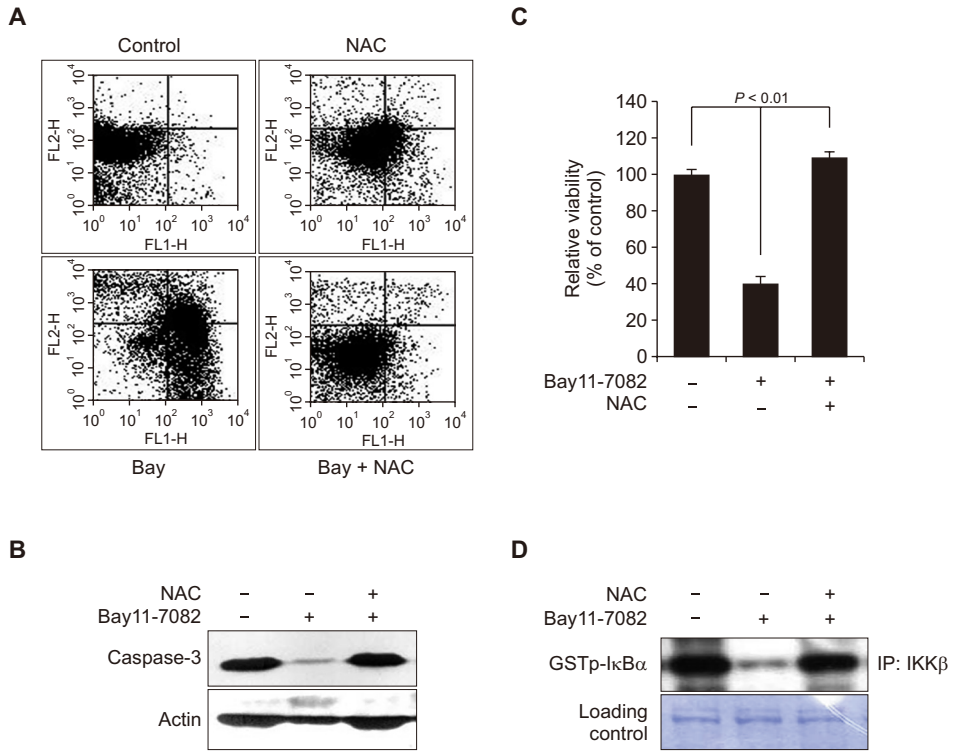

Figure 5. The IκB kinase (IKK) inhibitor Bay11-7082 induces apoptosis in MCF10A-*ras* cells. (A) MCF10A-*ras* cells were treated with Bay11-7082 (5 μM) for 24 hours in the absence or presence of *N*-acetyl-L-cysteine (NAC) (5 mM) to measure the Annexin V-FITC/propidium iodide positive cell population by flow cytometry. (B) MCF10A-*ras* cells were treated with the same IKK inhibitor for 24 hours, and the level of proteolytic cleavage of caspase-3 was determined by Western blot analysis. Actin was used as an equal loading control. (C) MCF10A-*ras* cells were treated with the IKK inhibitor in the absence or presence of NAC for 24 hours and cytotoxicity was measured by the MTT assay. (D). MCF10A-*ras* cells were treated with the IKK inhibitor for 12 hours, and the catalytic activity of IKK was determined by the kinase assay as described in Materials and Methods.

over, 9,10-dihydro-15d-PGJ_2 failed to suppress expression of IKKβ and to induce proteolytic cleavage of caspase-7 and PARP (Fig. 6F). These findings suggested that the C-9 position of 15d-PGJ_2 constituting the electrophilic α,β-unsaturated carbonyl group is essential for its pro-apoptotic activity.

DISCUSSION

We observed that 15d-PGJ_2 (10 μM) induced apoptosis in *ras* oncogene transformed human breast epithelial MCF10A cells, which was attributable to the ROS-mediated inhibition of catalytic activity of IKKβ and subsequently NF-κB signaling. 15d-PGJ_2 is characterized by the presence of a reactive α,β-unsaturated carbonyl group in the cyclopentenone ring. This moiety has been known to bind to sulfhydryl groups of cysteine residues of proteins by Michael addition, resulting in alteration of the protein structure and function [14]. 15d-PGJ_2 has been reported to direct modify the Cys 179 of IKKβ within their activation loop, thereby suppressing catalytic activity of IKK and transcriptional activity of NF-κB [17]. Consistent with this result, we observed that 15d-PGJ_2-induced suppression of catalytic activity of IKKβ and proteolytic cleavage of caspase 3 were attenuated in the MCF10A-*ras* cells harboring the mutant construct in which Cys 179 is replaced by alanine. In addition, the thiol reducing agent DTT attenuated the 15d-PGJ_2-induced suppression of IKK catalytic activity. Moreover, 9,10-dihydro-15d-PGJ_2 failed to induction of apoptosis and proteolytic cleavage of caspase-7 and PARP as well as DNA binding activity of NF-κB. Furthermore, we have observed that biotin-conjugated 15d-PGJ_2 directly binds to IKKβ. In line with our finding, Ciucci et al. [27] have shown that 15d-PGJ_2 inhibits the constitutive IKK and NF-κB activities in paclitaxel and doxorubicin-resistant estrogen receptor-negative breast cancer cells. 15d-PGJ_2-induced inactivation of NF-κB was followed by downregulation of NF-κB-dependent anti-apoptotic proteins, such as cIAPs1/2, Bcl-xL, and cellular

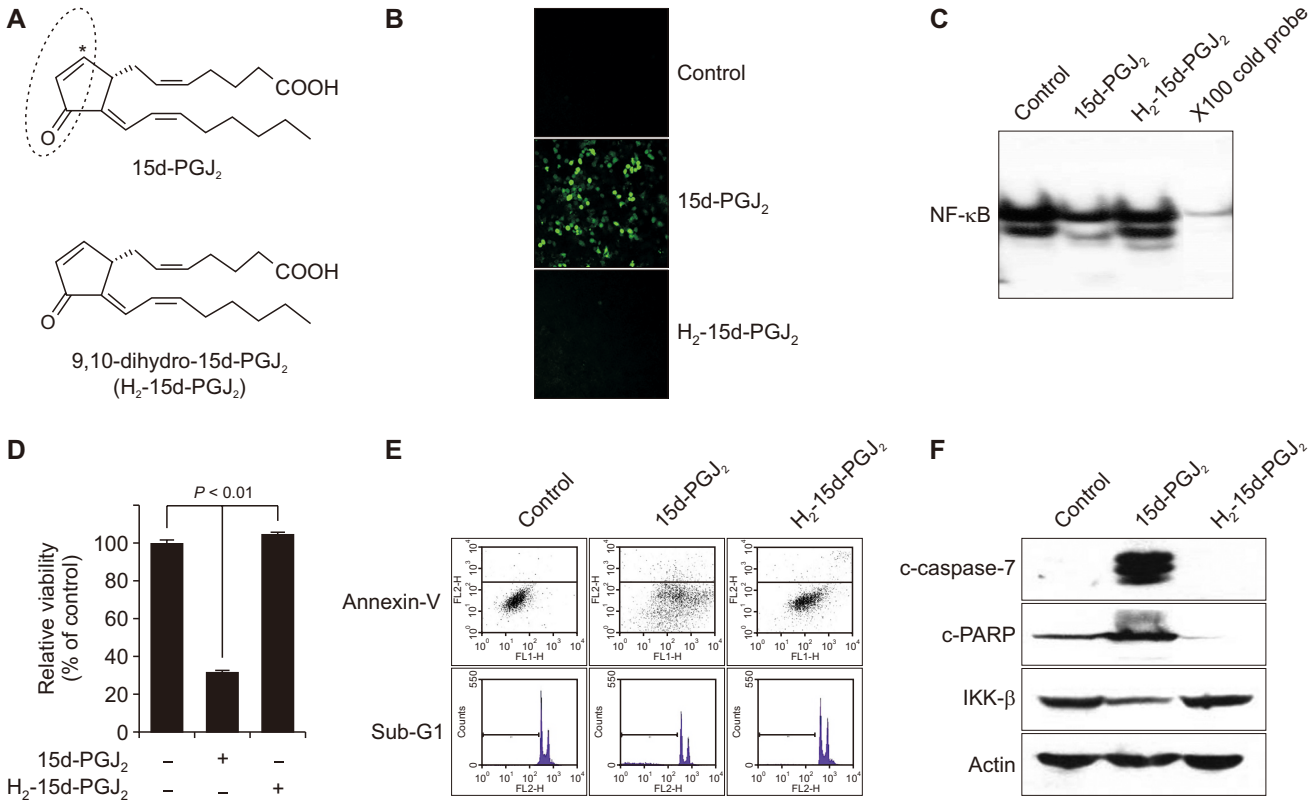

Figure 6. The cyclopentenone ring on 15-deoxy-$\Delta^{12,14}$-prostaglandin J_2 (15d-PGJ_2) is critical for 15d-PGJ_2-induced apoptosis in MCF10A-*ras* cells. (A) The chemical structures of 15d-PGJ_2 and its non-electrophilic 9,10-dihydro-15d-PGJ_2. An asterisk indicates an electrophilic carbon. (B, C) MCF10A-*ras* cells were treated with 15d-PGJ_2 (10 μM) or 9,10-dihydro-15d-PGJ_2 (10 μM) for 24 hours. Reactive oxygen species was measured by 2',7'-Dichlorodihydrofluorescein diacetate staining. (C) Nuclear extracts from MCF10A-*ras* cells were incubated with [γ-^{32}P]-labeled oligonucleotides harboring the NF-κB consensus sequence. The DNA binding activity were measured by electrophoretic mobility shifty assay. (D) MCF10A-*ras* cells were treated with 15d-PGJ_2 (10 μM) or 9,10-dihydro-15d-PGJ_2 (10 μM) for 24 hours, and cytotoxicity was measured by the MTT assay. Bars represent mean ± SE of three independent assays. A significant difference in the relative viability between treated cells and the solvent control is indicated with $P < 0.01$. (E) MCF10A-*ras* cells were treated with dimethyl sulfoxide, 15d-PGJ_2 (10 μM), or 9,10-dihydro-15d-PGJ_2 (10 μM) for 24 hours to measure the sub-G_0/G_1 population and the Annexin V-FITC/propidium iodide positive cell population. (F) The expression of proteolytic cleavage products of caspase-7 and PARP and that of IKKβ was determined by Western blot analysis in the MCF10A-*ras* cells treated for 24 hours with 15d-PGJ_2 (10 μM) or 9,10-dihydro-15d-PGJ_2 (10 μM).

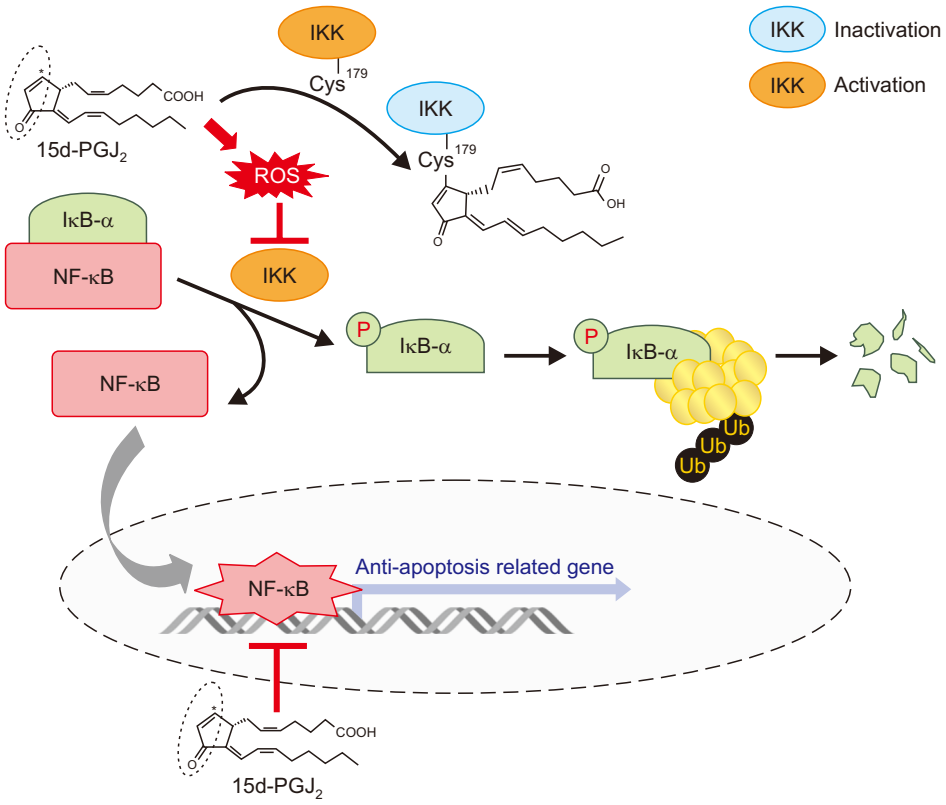

Figure 7. Proposed scheme on 15-deoxy-$\Delta^{12,14}$-prostaglandin J_2 (15d-PGJ_2)-induced suppression of IκB kinase β (IKKβ)–NF-κB signaling in MCF10A-*ras* cells.

FLICE-inhibitory protein, leading to caspase activation and induction of apoptosis [27]. In addition, Withaferin A from the Ayurvedic plant *Withania somnifera* has been known to directly inhibit IKKβ catalytic activity through modification of Cys 179, thereby exerting their chemotherapeutic activities [22]. 15d-PGJ_2 has been known to inhibit DNA binding of NF-κB by direct modification of Cys-62 of p50 [19]. Beside these residues of Cys, modification of Cys38 of p65 also plays an important role in suppression of NF-κB signaling and induction of apoptosis [28].

However, phosphorylation is critical mechanism to regulate NF-κB activation. Phosphorylation of two sites at the activation loop of IKKβ was essential for activation of IKK by tumor necrosis factor and interleukin-1 [29]. Oxidation or chemical modification of the thiols in the IKKβ and NF-κB can result in a conformational change and thus affection the phosphorylation. Thiol modification of IKKβ may induce its conformational change, which may prevent upstream kinase from phosphorylating the serine residues, thereby preventing activation of the complex [30]. Therefore, thiol modification of Cys179 of IKKβ can indirectly inhibit its kinase activity, resulting in suppression of NF-κB signaling.

We observed that ROS plays an important role in induction of apoptosis and nuclear translocation of p-p65 as well as suppression of IKKβ. Intracellular events associated with generation of ROS by 15d-PGJ_2 are likely to be a consequence of depletion of reduced glutathione and glutathione peroxidase and increased production of protein–bound lipid peroxidation products (e.g., 4-hydroxy-2-nonenal and acrolein) [31,32]. In addition, 15d-PGJ_2-inducd ROS generation is associated with reduction of thioredoxin (Trx) which plays an important role in the redox regulation of signal transduction and in cytoprotection against oxidative stress [33]. The overexpression of Trx protected against 15d-PGJ_2-induced apoptosis in human neuroblastoma SH-SY5Y cells. Further, 15d-PGJ_2 directly binds and modifies the Cys residues of Trx [33]. Consistent with these results, 9,10-dihydro-15d-PGJ_2 did not affect modification of Cys in Trx and inhibit the expression of epidermal growth factor receptor in oral squamous cell carcinoma [25]. Based on the previous studies, 15d-PGJ_2-induced disruption of mitochondrial membrane potential is attributed to disruption of redox homeostasis in MCF10A-*ras* cells.

In conclusion, 15d-PGJ_2 inhibited IKKβ activity, thereby inactivating NF-κB signaling in MCF10A-*ras* cells. 15d-PGJ_2-induced inhibition of NF-κB signaling and induction of apoptosis appear to be mediated by ROS and its covalent modification of IKKβ (Fig. 7).

ACKNOWLEDGMENTS

This work was supported by grants from Sungshin Women's University (2018-1-29-016).

CONFLICTS OF INTEREST

No potential conflicts of interest were disclosed.

ORCID

Hye-Kyung Na, https://orcid.org/0000-0003-0460-2810
Hongkyung Yang, https://orcid.org/0000-0002-4298-5632
Young-Joon Surh, https://orcid.org/0000-0001-8310-1795

REFERENCES

1. Li J, Guo C, Wu J. 15-Deoxy-Δ-^{12,14}-prostaglandin J2 (15d-PGJ2), an endogenous ligand of PPAR-γ: function and mechanism. PPAR Res 2019;2019:7242030.
2. Kim KR, Kim HJ, Lee SK, Ma GT, Park KK, Chung WY. 15-Deoxy-$\Delta^{12,14}$-prostaglandin J_2 inhibits osteolytic breast cancer bone metastasis and estrogen deficiency-induced bone loss. PLoS One 2015;10:e0122764.
3. Jang HY, Hong OY, Youn HJ, Kim MG, Kim CH, Jung SH, et al. 15d-PGJ_2 inhibits NF-κB and AP-1-mediated MMP-9 expression and invasion of breast cancer cell by means of a heme oxygenase-1-dependent mechanism. BMB Rep 2020;53:212-7.
4. Koma H, Yamamoto Y, Fujita T, Yagami T. 15-Deoxy-$\Delta^{12,14}$-prostaglandin J_2 enhances anticancer activities independently of VHL status in renal cell carcinomas. Biochem Biophys Rep 2019;18:100608.
5. Shin SW, Seo CY, Han H, Han JY, Jeong JS, Kwak JY, et al. 15d-PGJ_2 induces apoptosis by reactive oxygen species-mediated inactivation of Akt in leukemia and colorectal cancer cells and shows in vivo antitumor activity. Clin Cancer Res 2009;15:5414-25.
6. Cheng J, Nakamura H, Imanishi H, Liu W, Morisaki T, Sugiyama T, et al. Peroxisome proliferator-activated receptor γ ligands, 15-deoxy-$\Delta^{12,14}$-prostaglandin J_2, and ciglitazone, induce growth inhibition and cell cycle arrest in hepatic oval cells. Biochem Biophys Res Commun 2004;322:458-64.
7. Laurora S, Pizzimenti S, Briatore F, Fraioli A, Maggio M, Reffo P, et al. Peroxisome proliferator-activated receptor ligands affect growth-related gene expression in human leukemic cells. J Pharmacol Exp Ther 2003;305:932-42.
8. Chen YX, Zhong XY, Qin YF, Bing W, He LZ. 15d-PGJ_2 inhibits cell growth and induces apoptosis of MCG-803 human gastric cancer cell line. World J Gastroenterol 2003;9:2149-53.
9. Yen CC, Hsiao CD, Chen WM, Wen YS, Lin YC, Chang TW, et al. Cytotoxic effects of 15d-PGJ_2 against osteosarcoma through ROS-mediated AKT and cell cycle inhibition. Oncotarget 2014;5:716-25.
10. Hashimoto K, Farrow BJ, Evers BM. Activation and role of MAP kinases in 15d-PGJ_2-induced apoptosis in the human pancreatic cancer cell line MIA PaCa-2. Pancreas 2004;28:153-9.
11. Muhammad SN, Mokhtar NF, Yaacob NS. 15d-PGJ2 induces apoptosis of MCF-7 and MDA-MB-231 cells via increased intracellular calcium and activation of caspases, independent of ERα and ERβ. Asian Pac J Cancer Prev 2016;17:3223-8.
12. Sperandio M, Demasi APD, Martinez EF, Saad SO, Pericole FV, Vieira KP, et al. 15d-PGJ_2 as an endoplasmic reticulum stress manipulator in multiple myeloma in vitro and in vivo. Exp Mol Pathol 2017;102:434-45.
13. Tae IH, Park EY, Dey P, Son JY, Lee SY, Jung JH, et al. Novel SIRT1 inhibitor 15-deoxy-$\Delta^{12,14}$-prostaglandin J_2 and its derivatives exhibit anticancer activity through apoptotic or autophagic cell death pathways in SKOV3 cells. Int J Oncol 2018;53:2518-30.
14. Figueiredo-Pereira ME, Corwin C, Babich J. Prostaglandin J2: a potential target for halting inflammation-induced neurodegeneration. Ann N Y Acad Sci 2016;1363:125-37.
15. Pérez-Sala D, Cernuda-Morollón E, Cañada FJ. Molecular basis for the direct inhibition of AP-1 DNA binding by 15-deoxy-$\Delta^{12,14}$-prostaglandin J_2. J Biol Chem 2003;278:51251-60.
16. Kim EH, Surh YJ. 15-Deoxy-$\Delta^{12,14}$-prostaglandin J_2 as a potential endogenous regulator of redox-sensitive transcription factors. Biochem Pharmacol 2006;72:1516-28.
17. Rossi A, Kapahi P, Natoli G, Takahashi T, Chen Y, Karin M, et al. Anti-inflammatory cyclopentenone prostaglandins are direct inhibitors of IκB kinase. Nature 2000;403:103-8.
18. Straus DS, Pascual G, Li M, Welch JS, Ricote M, Hsiang CH, et al. 15-Deoxy-$\Delta^{12,14}$-prostaglandin J_2 inhibits multiple steps in the NF-κB signaling pathway. Proc Natl Acad Sci USA 2000;97:4844-9.
19. Cernuda-Morollón E, Pineda-Molina E, Cañada FJ, Pérez-Sala D. 15-Deoxy-$\Delta^{12,14}$-prostaglandin J_2 inhibition of NF-κB-DNA binding through covalent modification of the p50 subunit. J Biol Chem 2001;276:35530-6.
20. Na HK, Inoue H, Surh YJ. ET-18-O-CH3-induced apoptosis is causally linked to COX-2 upregulation in H-*ras* transformed human breast epithelial cells. FEBS Lett 2005;579:6279-87.
21. Galadari S, Rahman A, Pallichankandy S, Thayyullathil F. Reactive oxygen species and cancer paradox: to promote or to suppress? Free Radic Biol Med 2017;104:144-64.
22. Yang Y, Karakhanova S, Hartwig W, D'Haese JG, Philippov PP, Werner J, et al. Mitochondria and mitochondrial ROS in cancer: novel targets for anticancer therapy. J Cell Physiol 2016;231:2570-81.
23. Dai Y, Lawrence TS, Xu L. Overcoming cancer therapy resistance by targeting inhibitors of apoptosis proteins and nuclear factor-kappa B. Am J Transl Res 2009;1:1-15.
24. Ghosh S, Karin M. Missing pieces in the NF-κB puzzle. Cell 2002;109 Suppl:S81-96.
25. Yang J, Splittgerber R, Yull FE, Kantrow S, Ayers GD, Karin M, et al. Conditional ablation of Ikk*b* inhibits melanoma tumor development in mice. J Clin Invest 2010;120:2563-74.
26. Durand JK, Baldwin AS. Targeting IKK and NF-κB for therapy. Adv Protein Chem Struct Biol 2017;107:77-115.

27. Ciucci A, Gianferretti P, Piva R, Guyot T, Snape TJ, Roberts SM, et al. Induction of apoptosis in estrogen receptor-negative breast cancer cells by natural and synthetic cyclopentenones: role of the IκB kinase/nuclear factor-κB pathway. Mol Pharmacol 2006;70:1812-21.
28. Gupta SC, Kannappan R, Kim J, Rahman GM, Francis SK, Raveendran R, et al. Bharangin, a diterpenoid quinonemethide, abolishes constitutive and inducible nuclear factor-κB (NF-κB) activation by modifying p65 on cysteine 38 residue and reducing inhibitor of nuclear factor-κB α kinase activation, leading to suppression of NF-κB-regulated gene expression and sensitization of tumor cells to chemotherapeutic agents. Mol Pharmacol 2011;80:769-81.
29. Delhase M, Hayakawa M, Chen Y, Karin M. Positive and negative regulation of IκB kinase activity through IKKβ subunit phosphorylation. Science 1999;284:309-13.
30. Jeon KI, Byun MS, Jue DM. Gold compound auranofin inhibits IκB kinase (IKK) by modifying Cys-179 of IKKβ subunit. Exp Mol Med 2003;35:61-6.
31. Wang JJ, Mak OT. Induction of apoptosis by 15d-PGJ_2 via ROS formation: an alternative pathway without PPARγ activation in non-small cell lung carcinoma A549 cells. Prostaglandins Other Lipid Mediat 2011;94:104-11.
32. Ishii T, Sakurai T, Usami H, Uchida K. Oxidative modification of proteasome: identification of an oxidation-sensitive subunit in 26 S proteasome. Biochemistry 2005;44:13893-901.
33. Shibata T, Yamada T, Ishii T, Kumazawa S, Nakamura H, Masutani H, et al. Thioredoxin as a molecular target of cyclopentenone prostaglandins. J Biol Chem 2003;278:26046-54.